Pencil Beam Studies of Low Mass Stars in the MUSYC Survey

Martin Altmann(1), Rene Mendez(1), Vladimir Kochargin(2), Bill van Altena(2), Maria-Teresa Ruiz(2), Eric Gawiser(2) & MUSYC

1: Departamento De Astronomia, Universidad de Chile, Camino Del Observatorio 1515, Las Condes, Chile
2. Astronomy Department, Yale University, 260 Whitney Avenue, New Haven CT06520, USA

0.1 The MUSYC Galactic Programme

Here we present the results of star count studies in three of the four MUSYC fields. MUSYC, the MUltiwavelength Survey by Yale Chile (see Gawiser et al. 2006 or `http://www.astro.yale.edu/MUSYC`) is a one square degrees deep multipassband (UBRVIzJHK) survey, mainly conducted by institutions in Chile (Universidad de Chile and P. Universidad Catolica) and Yale University in the USA, as well as many other partners in the world. While mostly aiming at extragalactic science, MUSYC also has a Galactic programme - this involves multi epoch imaging of the four MUSYC fields, as well as of field from a previous effort (The CYDER fields, now known as MUSYC extended) for a larger field coverage. The main aim of the Galactic programme of MUSYC is to find and census White and Brown dwarfs, both of which are intrinsically very faint and hence relatively close objects, which should reveal themselves by their large proper motion. Knowing the density of White Dwarfs, which are rather massive faint objects, would enable one to determine their fraction making up baryonic dark matter. Moreover, finding cool and ancient WDs allows to set constraints on the age of the stellar component of our MW. Little is also known about the space density of Brown Dwarfs. The data taking for the second epochs has just been completed after having been delayed for more than 2 years by adverse weather conditions and technical issues.

A third issue is Galactic structure and the distribution of normal main sequence stars along our pencil beams. For 3 of the 4 Generic MUSYC fields (Cast 1255+01 has the final photometry not yet available), i.e. CDFS-Ext (iα=03:32:29, δ=$-$27:48:27, l=223, b=-54), SDSS 1030+05 (10:30:27, +05:24:55, 240, +50) and HDFS-Ext (22:32:35, -60:47:12, 328, -50) we have studied the distribution of lower main sequence stars along the pencil beams defined by these fields. We were able to clearly discern a Halo and a Thick Disk component, the Thin Disk being only visible in CDFS-E, were the upper magnitude cutoff is at far brighter magnitudes (The data for CDFS-E comes from the smaller 2.2m ESO telescope/WFI rather than MOSAIC2 at the 4m Blanco at CTIO).

0.2 Defining our Sample

In order to achieve a clean and as complete as possible star sample we first sorted out all non-point source object by using the CLASS parameter of SExtractor. The limit we used was 0.85. As indicated by studies performed on MUSYC data the CLASS index is reliable until about 25 mag and breaks down at 26. However the point sources seem to go to about 25.5 without significant incompleteness, the completeness breaking down at 26.5 mag. Our K- and M-stars have a different magnitude distribution at faint magnitudes than the other point sources - which are dominated by faint AGNs and

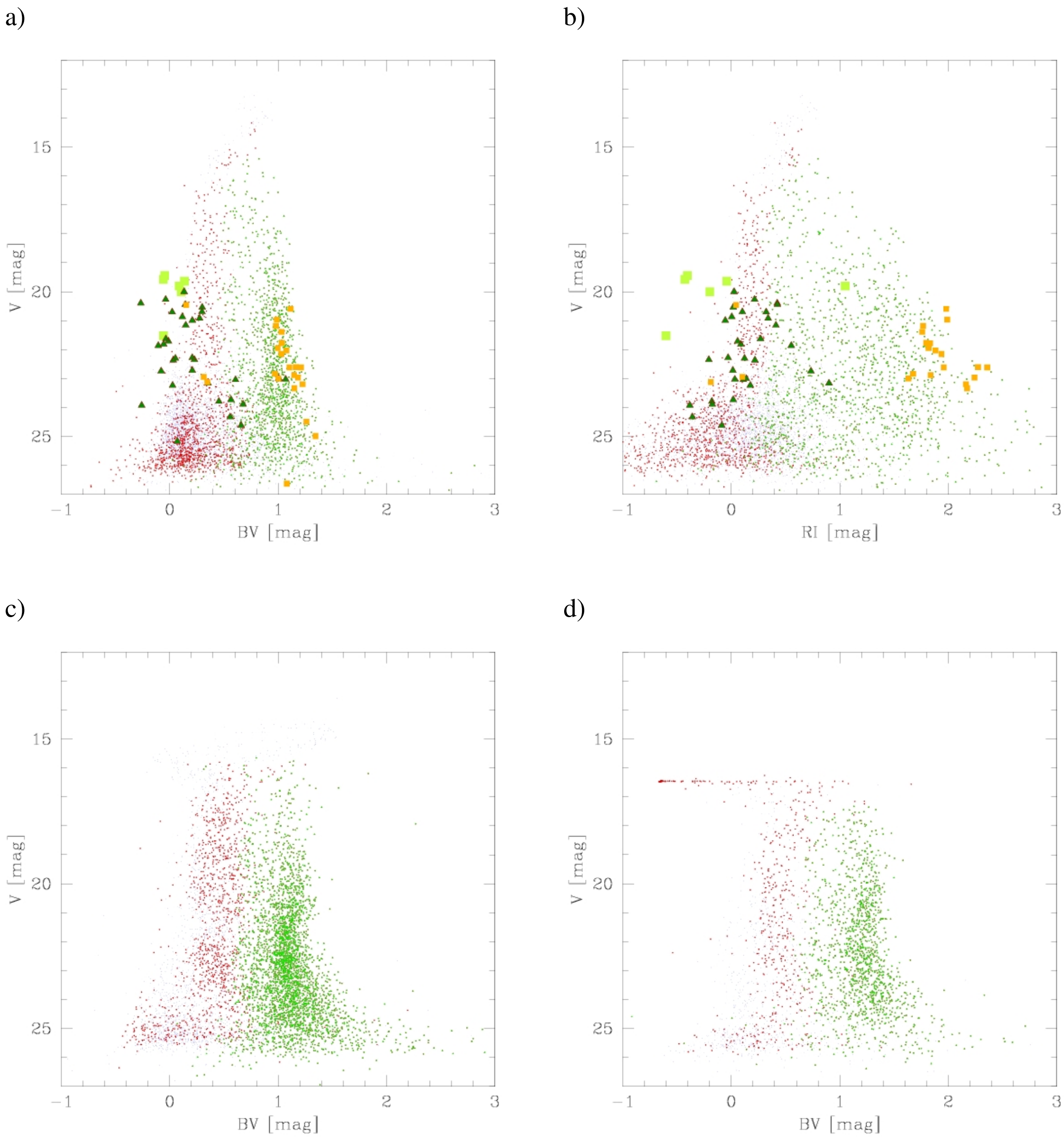

Figure 1: Colour magnitude diagrams of our three fields. Blue dots denote all point sources, red dots those classified as stars by our SED fitting routine, green dots are the stars of our samples.
a) and b) CDFS-E (a) is V vs. $R - I$, b) V vs. $B - V$), larger symbols show spectroscopically classified objects, purple triangles are AGNs, lime squares show WDs, orange squares other stars.
c) and d) are CMDs (V vs. $B-V$) of HDFS-E and 1030+05 respectively - note the signs of saturation at bright magnitudes in contrast to CDFS-E.

other extragalactic objects (see Fig. 1).

The second step was to classify all objects in the point source catalogue by using their SED as measured by the multi passband photometry. This was accomplished by a routine which

a) b)

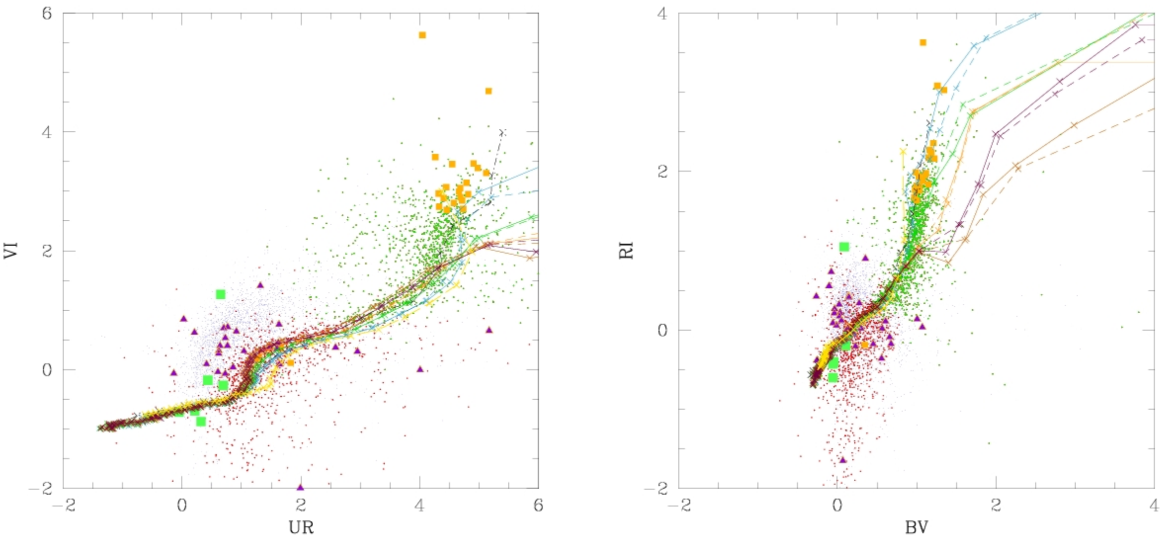

Figure 2: Colour-Colour Diagrams of CDFS-E:
a) V-I vs. U-R, b) R-I vs. B-V. The symbols are the same as in Fig. 1. The tracks show BaSel main sequence tracks (solid: logg=4.0, dashed: 4.5) for [Fe/H]s of 0,-0.5,-1,-1.5,-2 (blue to brown tracks), as well as one track of solar metallicity subgiants (yellow, long dashes). Note that the blue main sequence most closely follows metalpoor tracks, while most red stars favour the tracks of solar and -0.5 metallicity. The subgiant track is almost unpopulated.

1. convolves spectral flux templates by the filter, detector and atmosphere functions and
2. fits the photometric fluxes to the convolved template fluxes, classifying an object by minimising the χ^2.

The normalisation factor between observed flux and template is determined analytically. Since extragalactic objects and stars show significant overlap in the bluer part of the stellar main sequence, i.e. in the spectral types F and G, we chose to restrict ourselves to the lower main sequence stars, i.e. those with temperatures below 5000 K. In this region there is little or no contamination, as can be seen from those objects for which we have spectra, some 30-40 in all fields. All of them are either stars or not classifiable due to low S/N in the spectra (see Fig. 1a+b, 2). For the SED fitting we used templates from the BaSel-2.2/3.1 libraries for stars (Westera et al. 2002), and adapted as well as redshifted and extinction corrected extragalactic templates. Our final selection delivers about 1400 stars in CDFS-E and 1030+01 but 3400 in HDFS-E. This larger star density is already obvious from the colour magnitude diagrams of this field (see Fig. 1c).

0.3 Correcting the Sample for Completeness, Metallicity, etc.

Before we can proceed to study the distribution, we need to correct our samples for various effects, which affect and alter the samples.

Reddening could play an important role - however these fields were chosen so that they have negligible reddening. Therefore we can safely ignore the effects of Galactic reddening - normally this effect needs to be taken care of before the SED fitting, since it can potentially severely alter the outcome of that process.

Abundance variations do alter the relation between colour and luminosity, which needs to be corrected. While the BaSel libraries give us a metallicity (Fig. 2), we decided to follow the approach of Siegel et al. (2002), i.e. assigning metallicities to the stars according to their distance to the Galactic plane. Their relations have been verified by several empirical studies, and is well suited for our large samples.

Our samples are also affected by luminosity dependent incompleteness. Stars of the lower main sequence span several magnitudes in absolute brightness. Hence our sample covers different distance ranges depending on the colour, i.e. luminosity. To achieve unbiased samples, we need to correct this. In this case we used a method derived by Phleps et al. (2000,2005). This method divides the sample into logarithmic distance bins, and adds the missing" stars (i.e. those that are fainter than the detection limit of each bin) into the more distant bins.

Another potential point of concern is subgiant contamination. Given the depth of our samples, we expect this contamination to be low. In fact, our colour-colour diagram shows only very few, if any objects following a giant track. Therefore we have chosen to neglect subgiant contamination (see Fig. 2b). Phleps et al. (2000), working in a similar magnitude range also reasoned that SG-contamination was negligible.

Finally, one needs to take into account the effects of binarity. Many stars are binaries - binarity puts a given object of a given colour/temperature further away, since it seems to be brighter than an individual star of the same type would be. Solar type stars have a binary fraction of about 50whether this also holds true for a) low mass stars and b) Halo stars. Many studies come to the conclusion that the fraction of binaries is significantly lower. Nonetheless the effect binarity has on the results of this undertaking needs to be explored. While this is still pending, we plan to analyse the effect of 30of double stars. The magnitudes and colours of each component will be considered to be equal, since objects of significantly different colours will also be of very different luminosity, the secondary thus being more and more insignificant. On the whole, according to Siegel et al. (2002) the effect stellar binarity has on the distribution of stars is not very large.

After correcting for all these effects, we can now go ahead and calculate the photometric parallaxes and derive the distributions of our stars.

0.4 Photometric Parallaxes and Normalisation by Volume

Having accounted for possible adverse effects, we finally have clean and complete samples for our three fields. Now we need to derive the distances of the stars by using photometric parallaxes. For this we need a good colour-absolute magnitude relation. The relation published in Lang (1992) does not go to cool enough stars - moreover it can today be regarded as obsolete. The most reliable such relations are those derived empirically by the RECONS project (Henry et al. 2004). Unfortunately these are given as M_K(colour ind). Therefore we had to tranform them to $M_R(R-I)$ before we could use them. To accommodate for metallicity we used the relation:

$$M_R([Fe/H] = -0.625 * [Fe/H] + M_R \qquad (1)$$

This fits very well to the results of the study of the low mass subdwarf luminosity function by Gizis et al. (1997) in the interval where the latter applies. Our final $M_R(R-I)$ relation was parameterised

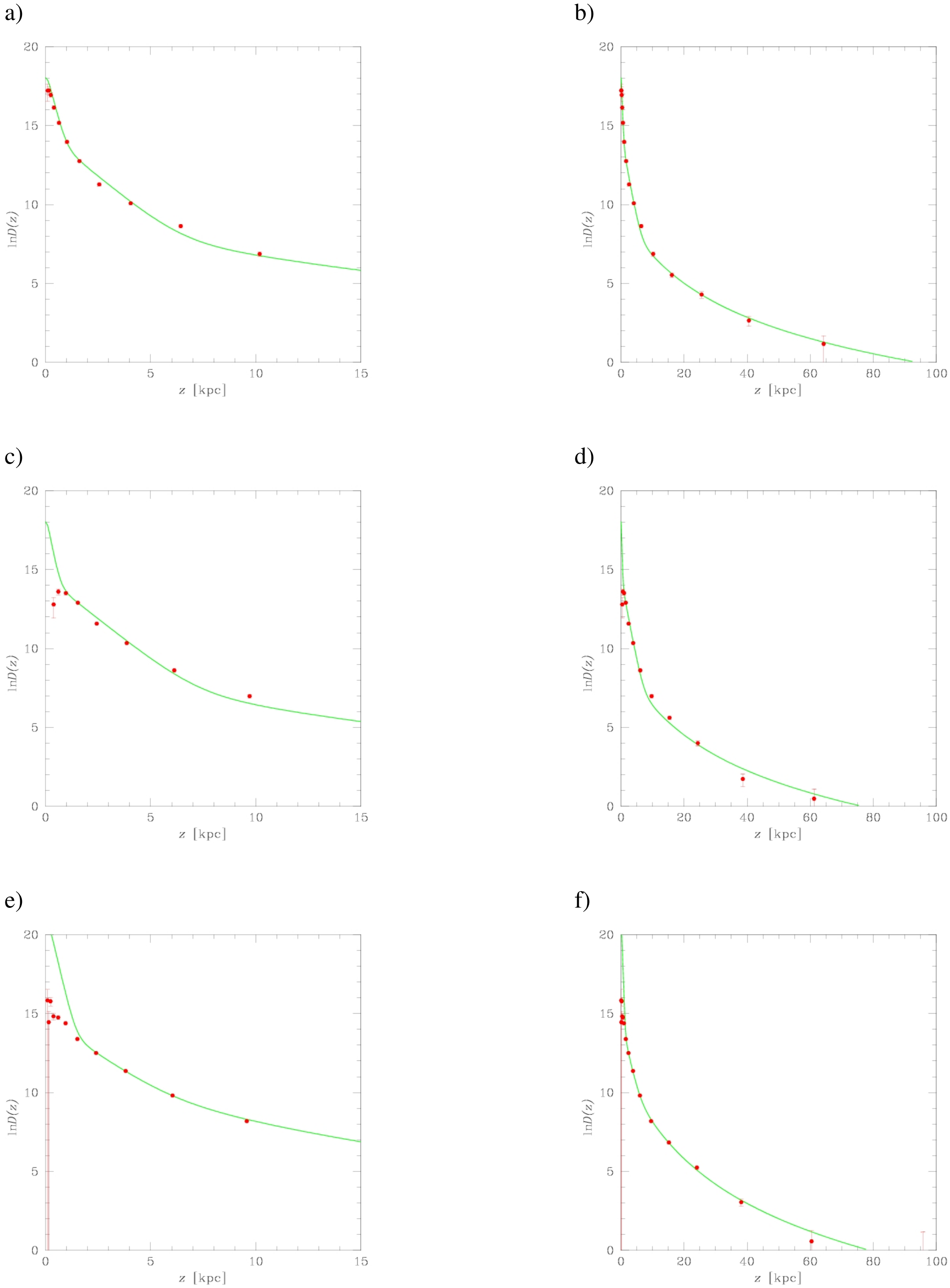

Figure 3: The z-distributions of the lower main sequence stars of our fields. a), c), and e) show the inner 15 kpc, b), d), and f) the outer distribution up to 100 kpc. a), b): CDFS-E, c),d): 1030+05, e), f): HDFS-E. The errorbars are mostly smaller than the symbols.

by a 5th order polynomial and is valid for $R - I$ between 0.15 and 2.5. The few stars redder than $R - I$=2.5 are expunged from our sample - they (stars near the star-BD border) are intrinsically so faint, that they contribute almost nothing to our sample - their distance range being less than 100 pc.

Finally, the bins have to be normalised by their volume. For this the count number in each bin is divided by the volume of the bin, derived by the according formula for a truncated tetrahedron.

0.5 The Results: Scale Heights for the Disks and a Power Law Exponent for the Halo, Density Quotients, and Discussion

To characterise our distribution, which (in the case of CDFS-E) clearly consists of three distinct components, we fitted a function consisting of two exponentials and a power law to the data using Gnuplot. These three functions each represent a Galactic component, i.e. the Thin and Thick Disk as well as the Galactic Halo. Before fitting, we adjusted the bins for Galactic latitude, i.e. $z = d|\sin b|$. For CDFS-E, the field with the brightest bright magnitude cutoff we determined the scale height of the Thin Disk to be 180 pc - please note however that this result should be regarded with some caution, since there may be a number of stars missing due to saturation, even although saturation unlike in the case of the other two fields was not obvious from the CMD. The scale height of the Thick Disk in the CDFS-E beam was determined to be 915 pc, its density relative to the Thin Disk at z=0: 3Halo was found to have a power law falloff coefficient of -3.44 and a relative density at the galactic plane of 0.006fields the region where the Thin Disk dominates was underpopulated (see above), so that we could not derive meaningful values for this component. We nonetheless left the Thin Disk as a free parameter in the fit and the results did not change significantly. For SDSS 1030+05 we found a Thick Disk scale height of 950 pc, a Halo falloff exponent of -3.60 and a relative local density of the Halo of 0.1Thick Disk. For HDFS-E the values are 1075 pc, -4.52 and 0.1the Halo can be traced to galactocentric distances of more than 100 kpc (see Fig. 3).

The value for the Thin Disk scale height is a bit lower than the canonical value for the old disk. The reasons could be a mixture of old and young stars, as well as completeness problems at the bright end. The scale height of the Thick disk has been subject to great controversy with values ranging from 600 to 1700 pc. However the most recent results seem to converge at values between 800 and 1100 pc, well in line with our result. About 900 pc is the result of the studies of amongst others Altmann et al. (2004), Phleps et al. (2005), and Cabrera-Lavers et al. (2007), invoking very different techniques and approaches. The latter also found a dependency of the scale height with l, which seems to be confirmed by our results, with the sest to l=0 having the largest scale height. The falloff exponent of the halo agrees well in two of the fields, and is close to the canonical value, the value for HDFS-E is much larger - this is presumably caused by the more dense Thick disk in this field pointing almost directly above the Gal. Centre. Further steps in the analysis include, fitting a flattened and even triaxial Halo to our data.

Acknowledgements:

This work is supported by FONDAP centre for excellence in Astrophysics 1501 0003 (MA, RM and MTR), MA acknowledges travel support by the Deutsche Forschungsgesellschaft (DFG) and support by the LOC of the Bonn MW Halo conference. EG is supported by a NSF grant. We would like to thank the NOAO TAC, ESO OPC, and CNTAC for the generous granting of observing time, as well as the staff of the according observatories for supporting our observations. We have made significant use of internet based databases, such as SIMBAD, NED, VIZIER, ALADIN, DSS etc.

References:

- Altmann, M., Edelmann, H., de Boer, K.S., 2004, A&A 414, 181
- Cabrera-Lavers, A., Bilir, S., Ak, S., Yak, E., Lopez-Corredoira, M, 2007, A&A 464, 565
- Gawiser, E., van Dokkum, P., Herrera, D., ..., Altmann, M., et al., 2006 ApJS 162, 1
- Gizis, J.E., 1997, AJ 113, 806
- Henry, T.J., Subsavage, J.P., Brown, M.A., et al., 2004, AJ 128, 2460
- Lang, K.R., 1992, "Astrophysical Data I", Springer Verlag, Berlin
- Phleps, S., Meisenheimer, K., Fuchs, B., Wolf, C., 1998, A&A 356, 108
- Phleps, S., Drepper, S., Meisenheimer, K., Fuchs, B., 2005, A&A 443, 929
- Siegel, M.H., Majewski, S.R., Reid, I.N., Thompson, I.B., 2002, ApJ 578, 151
- Westera, P., Lejeune, T., Buser, R., Cuisinier, F., Bruzual, G., 2002, A&A 381, 524